ISSN No. 2395-0900
International Journal of Engineering Studies and Technical Approach
IJESTA

Templaste and Inasu algorithms using Medical images Analysis

Prof P. Senthil

Associate professor in MCA Computer Science,Kurinji College of Arts and Science, Tiruchirappalli

ABSTRACT

This paper functions a hardware application for coaching of neural networks victimization optical correlation. Among the assorted neural network architectures Cellular Neural Network (CNN) is chosen as a result of its image process capability. CNNs need rather more computation throughout the coaching stage compare to check method. To decrease the coaching method time and to implement in hardware, optoelectronic design is developed during this study. Optical design offers parallel Inasu algorithms Using high speed process capability for second processing applications. Optical Correlation employs lens and CCD cameras with shaft of light that understand second matrix operation and summation within the speed of light. Therefore, within the every iteration of coaching, optical correlation handles additional computation burden inherently and therefore the remainder of mathematical computation completed digitally.

Keywords: *CNN training, optoelectronic hardware, Inasu algorithm, Speed,Templaste.*

I.INTRODUCTION

A cellular neural network (CNN) is a synthetic neural network that options a multi-dimensional array of neurons and native interconnections among the cells. The original CNN paradigm was 1st projected by Chua and principle in 1988. the 2 most basic ingredients of the CNN paradigm are: the utilization of analog process cells with continuous signal values, and native interaction at intervals a finite radius. A CNN may be a nonlinear analog circuit that processes signals in real time. it's product of an enormous combination of frequently spaced cloned circuit, known as cells, that communicate with one another directly solely through their nearest neighbors. 1) Learning algorithms, 2) Hardware implementation, and 3) Application to various engineering and scientific problems. Among the various hardware implementations, Kowalski et. al. reported programmable weighted order statistic image filters based CNN architecture [3]. It is a kind of development of the CNN-based analog VLSI circuit. Arena et al. presented a real-time object oriented segmentation algorithm, designed and implemented on a new type of mixed analog/digital chip based on the cellular neural network [4]. Hung et al. developed a multifunction optoelectronic cellular neural network combining an electronic CNN and metal-semiconductor-metal photodiodes [5]. Each above hardware implementations have been presented as alternative applications. However, all of them have been realized for test stage of CNN. CNN applications require massive mathematical computation due to the operations of summing cross-correlations of bipolar input and state data[6]. Especially, in the training stage this recursive operation of summing cross-correlations increase computational expenses[7]. Although these mathematical operations are easy to implement in software, they are very burdensome in the hardware implementations and therefore more costly[8]. A common principle for all hardware implementations is their simplicity[9]. Therefore, hardware-friendly training algorithms are

preferred to ensure the functionality and cost effectiveness of the CNN's hardware implementation. In this study, a hardware-friendly supervised learning algorithm has been used by modifying Widrow-hoff learning algorithm[10].

The optoelectronic hardware implementation of the training stage for CNN has been designed using well known optical correlation technique[11], joint transform correlator (CST)[12].Parallel operations capability of the CST can potentially provide high computational power at a limited cost, thus, can potentially solve a massive computation problem in the training period[13]. However, realization of templates coefficients and pixel values are a problem for classical (amplitude-only) CST due to consisted negative values[14]. To alleviate this problem, phase-only joint transform correlator technique has been used, in which both the input and Fourier planes are phase-encoded[15]. Thus, it allows the encoding of bipolar data (including positive and negative values) in the input plane unlike the amplitude-only CST[16].

For two operations of summing-cross-correlation are performed by multi-object input joint image. In the output plane of the multi-object CST, the correlation terms for each object is generated as separate and non-overlapping distributions. Thus, multiple correlations are performed simultaneously in one step[18-23].

RESEARCH METHODOLOGY

In **solving partial differential equations**, CNN is suitable for reducing non-visual problems to geometric maps for

- thermographic maps
- antenna-array images
- medical maps and images

I.INASU ALGORITHMS

Input: U(t) = static binary image ;

Initial state: X(0) = arbitrary (reason: Feedback Templaste = 0)

Output: Y(t) converges toward a binary image showing all edges of the input image.

```
numObs = length(species);
p = randperm(numObs);
meas = meas(p,:);
species = species(p);
half = floor(numObs/2);
training = meas(1:half,:);
trainingSpecies = species(1:half);
sample = meas(half+1:end, Templaste:);
grouphat = classify(sample,training,trainingSpecies);
CellRow=4;% the number of row of cells
CellCol=4;% the number of colume of cells
r=1;
```

```
A=[0 1.0 0; 1.0 2.0 1.0; 0 1.0 0];
B=[0 zero zero; zero zero zero; 0 0 0];
I=[0 zero zero zero; zero zero zero zero; zero zero zero zero; 0 0 0 0
Initials=[-0.8 1.0 -1.0 -0.6; 1.0 1.0 1.0 -1.0; -1.0 0.9 -1.0 -0.8; -0.9 -1.0 -0.7 -0.8]; this first states
[Arow Acol]=size(A); range in size of CNN
[Brow Bcol]=size(B); to notice that sizes of A and B ar equal
for i=1:CellRow
for j=1:CellCol
for n=1:Arow
for m=1:Acol
comm=sprintf('set_param("Cellmodel/CST","value","%.3f")',i,j,n,m,A(n,m));
eval(comm);
comm=sprintf('set_param("Cellmodel ","value","%.3f")',i,j,n,m,B(n,m));
eval(comm);
end
comm=sprintf('set_param("Cellmodel/C ","value","%.3f")',i,j,I(i,j)); absolute bias/sources
eval(comm);
comm=sprintf('set_param("Cellmodel/C,"Initial","%.3f")',i,j,Initials(i,j));% Initial States to cells
eval(comm);
end
sim('Cellmodel');
Output of CNN
Final_State_ofCNN
s11(lastpoint)+s12(lastpoint)+s13(lastpoint)+s14(lastpoint);
s21(lastpoint)+s22(lastpoint)+s23(lastpoint)+s24(lastpoint);
s31(lastpoint)+s32(lastpoint)+s33(lastpoint)+s34(lastpoint);
s41(lastpoint)+s42(lastpoint)+s43(lastpoint)+s44(lastpoint)]
disp('Plot the transient of C(2,2) as shown in Figure 9d');
```

CNN Architecture

Cellular neural network includes analog, nonlinear, dynamic processing elements called cell, which are locally inter-connected. The basic cell architecture is shown in Fig. 1. In contrast the feed forward neural network, CNN employs two template matrices that are a form of fix sized masks. A CNN is entirely characterized be a set of nonlinear differential equations associated with the cells. The adjacent cells can interact directly with each other. Cells not directly connected together may affect each other indirectly because of the propagation effects of the dynamics of CNNs.

ISSN No. 2395-0900
International Journal of Engineering Studies and Technical Approach
IJESTA

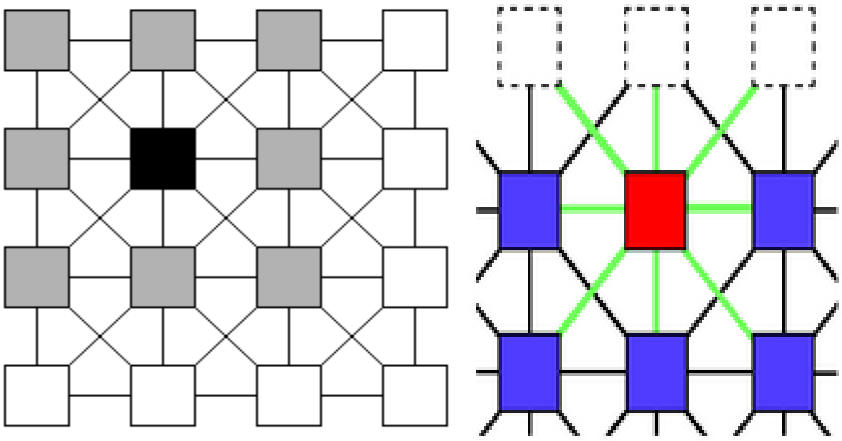

Fig. 1 The basic cell architecture of cellular neural network.

Each cell includes input, state, and output variables denoted by *u*, *x*, and *y*, respectively. Every cell is influenced by a limited number of cells in its environment. This locality of connections between the units is the main difference between CNNs and other neural networks. Large CNN chips can be implemented using VLSI techniques. The figure above shows the emphasized cell (black) connected to the nearest neighbors (gray). The cells marked in gray represent the neighborhood cells of the black cell. The neighborhood includes the black cell itself. This is called a "3*3-neighborhood". Similarly, we could define a "5*5-neighborhood", a "7*7-neigborhood" and so on.

The state and the output equations of a discrete time CNN can be written as follows

$$x_{i,j}(n+1)+Q(CS)=\sum_{m=-s}^{s}\sum_{n=-s}^{s}A_{m,n}\,y_{i+m,j+n}(n)+\sum_{m=-s}^{s}\sum_{n=-s}^{s}B_{m,n}\,u_{i+m,j+n}(n)+I+TW(Q) \quad (1)$$

$$y_{i,j}(n+1)=f[x_{i,j}(n+1)]=\frac{1}{2}\left(\left|x_{i,j}(n+1)+1\right|-\left|x_{i,j}(n+1)-1\right|\right) \quad (2)$$

where matrices $A_{m,n}$ and $B_{m,n}$ represent the set of coefficients which weight the influence of the outputs and inputs of the neighboring cells into the state of the cell under consideration. In this study, 3x3 sized template matrices are required to approach all operations. The completely stable CNNs can operate either in the bipolar binary steady-state output mode or in the real valued steady-state output mode. The first mode type CNN is selected in this work that the input and the steady-state output is defined as {-1, 1}.

Optoelectronic Correlation Architecture

In the literature, two type optical correlation architectures are well known which are the Wanderlust correlation and joint transform correlation. CST has been attractive technique in various fields. The classical CST, which is known amplitude-only CST, performs cross correlation between an input and a reference images placed into input joint image. The input joint image with *n* objects are displayed on the SLM (spatial light modulator) and can be described as follows

$$r(x,y)=\sum_{i=1}^{n}t_i\,(x-x_i\,,y-y_i\,) \quad (3)$$

ISSN No. 2395-0900
International Journal of Engineering Studies and Technical Approach
IJESTA

where t_i represents each object in the input joint image. In the CST architecture, the light beam emanating from the laser is collimated by a collimating system which consists of a microscopic objective and one lens. The collimated light beam illuminates the SLM where the input joint image is displayed. The second lens performs Fourier transform of the input joint image, and the corresponding joint power spectrum (JPS) captured by the square-law detector CCD camera is given by,

$$|R(u,v)|^2 = \sum_{i=1}^{n} |T_i(u,v)|^2 + 2\sum_{i=1}^{n}\sum_{\substack{k=1 \\ k\neq i}}^{n} |T_i(u,v)|\,|T_k(u,v)| \cos[\phi_{ti}(u,v) - \phi_{tk}(u,v) - ux_i + ux_k - vy_i + vy_k] \quad (4)$$

where $|T_i(u,v)|$ is the amplitudes and $\phi_{ti}(u,v)$ is the phase of the Fourier transform of $t_i(x,y)$; u and v are frequency-domain variables. The first term is called zero order term, and the second term is called desired cross-correlation between the multi-object in Eq (4).

Optoelectronic Hardware Architecture

Convergence to stable state of CNN depends on the suitable template coefficients and bias values inside the cells. The objective to obtain suitable template coefficients depends on the learning algorithm that is used to convergence input-output map by adjusting the template coefficients. The dynamic architecture of CNN is a drawback to use any supervised learning algorithm properly. That's why, initially the learning algorithm should be designed for CNN structure. In this paper, perception based structural approach is developed to modify Windrow learning rules into the traditional CNN as shown in Fig. 2.

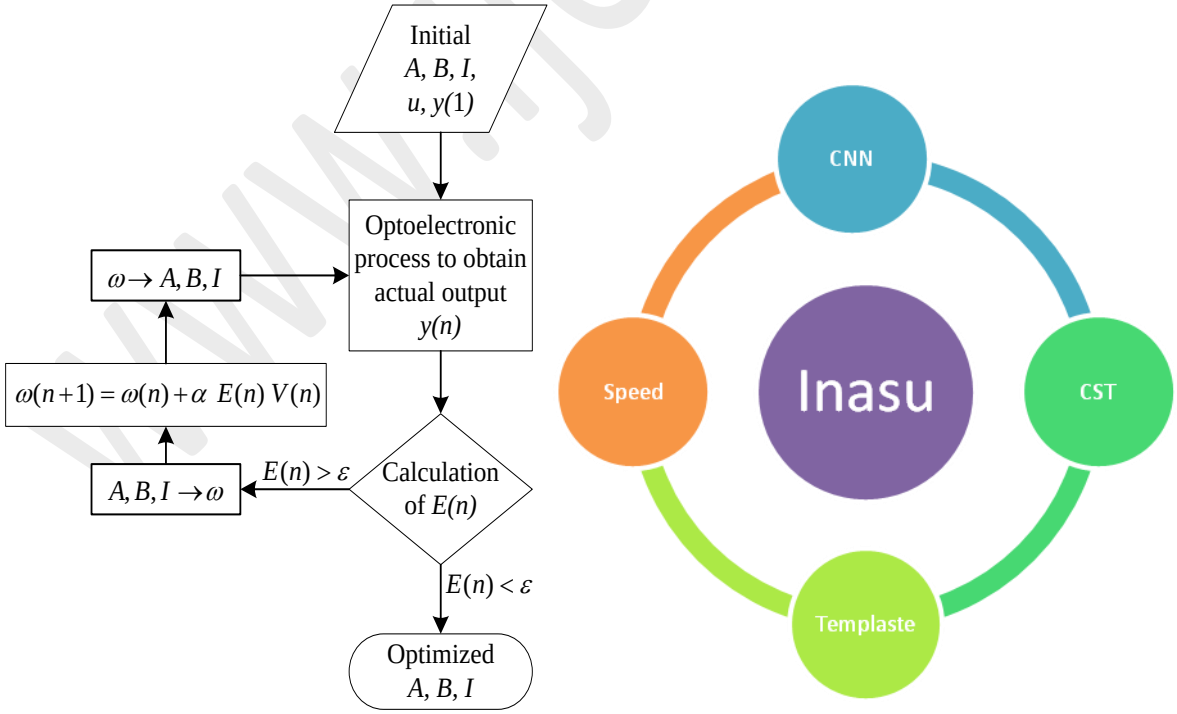

Fig. 2 Flow chart Inasu algorithm.

ISSN No. 2395-0900
International Journal of
Engineering Studies and Technical Approach
IJESTA

Initially, template matrices are converted to weight vector form of ω. Then, updated weight coefficients in Widrow rules is defined, for CNN as follows

$$\omega(n+1) = \omega(n) + \alpha\ E(n)\ V(n) \tag{5}$$

where α is the learning rate, $V(n)$ is input vector, $E(n)$ error function, and $\omega(n)$ is the weight vector at iteration n. The error function in Eq. (5) can be defined as a difference between actual output y and desired output d,

$$E(n) = \frac{1}{2}\sum (y(n) - d)^2 \tag{6}$$

To converge actual output y requires so many iterations during the learning period. Since two summing cross-correlation operations in Eq. (1) causes computation burden in the each iteration, these operations are carried by the optic implementation. The rest of simple summation processes are achieved by digitally.

The CST architecture is designed for multi-object input joint image that performs multiple correlations simultaneously. The multi-object input joint image generates cross correlations either separate or overlapping distributions according to set up of input joint image. This feature provides significant advantages to realize high speed multi cross-correlations in one step as simultaneously [7,8].

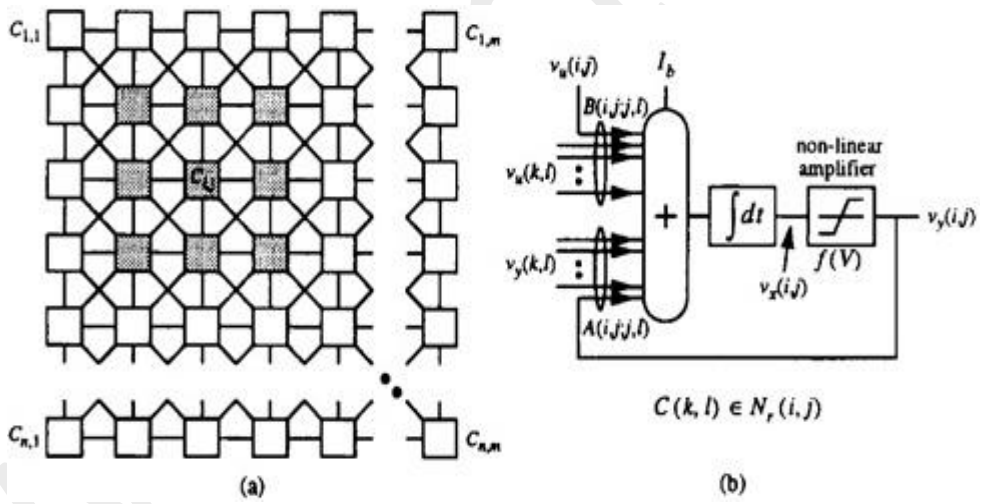

Fig3.(a) Processing in CNN (b) Execute in CNN

In the training stage, overlapped output image is desired in the correlation output corresponding to summation of two correlation terms in Eq. (1). Each term in Eq. (1) is considered as an object in the multi-object input joint image. The input image u and output image y are placed at the top-half of the input joint image, while the two template matrices (B and A) are displayed at the bottom half. The corresponding multi-object input joint image can be expressed as

$$r(x,z) = u(x+x', z-z') + y(x-x', z-z') + B(x+x', z+z') + A(x-x', z+z') \tag{7}$$

International Journal of Engineering Studies and Technical Approach
IJESTA
ISSN No. 2395-0900

TEMPLASTE DIFFERENTIAL EQUATION:

$$C\frac{dx_{ij}}{dt} = -\frac{1}{R}x_{ij} + \sum_{k}(a_k y_k + b_k u_k) + 1$$

k denotes the neighborhood of the specific cell

Without loss of generality, the time constant T = R*C can be set to 1.
The only **nonlinear element** in each cell is a piecewise-linear voltage controlled voltage source with characteristic

$$y(i,j) = f(x(i,j)).$$

A widely used nonlinearity is the piecewise-linear function as given by:

$$y(i,j) = f(x(i,j)) = 0.5*(|x + 1| - |x - 1|)$$

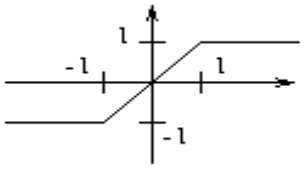

Fig.3AThe CNN of a cell C(i,j)

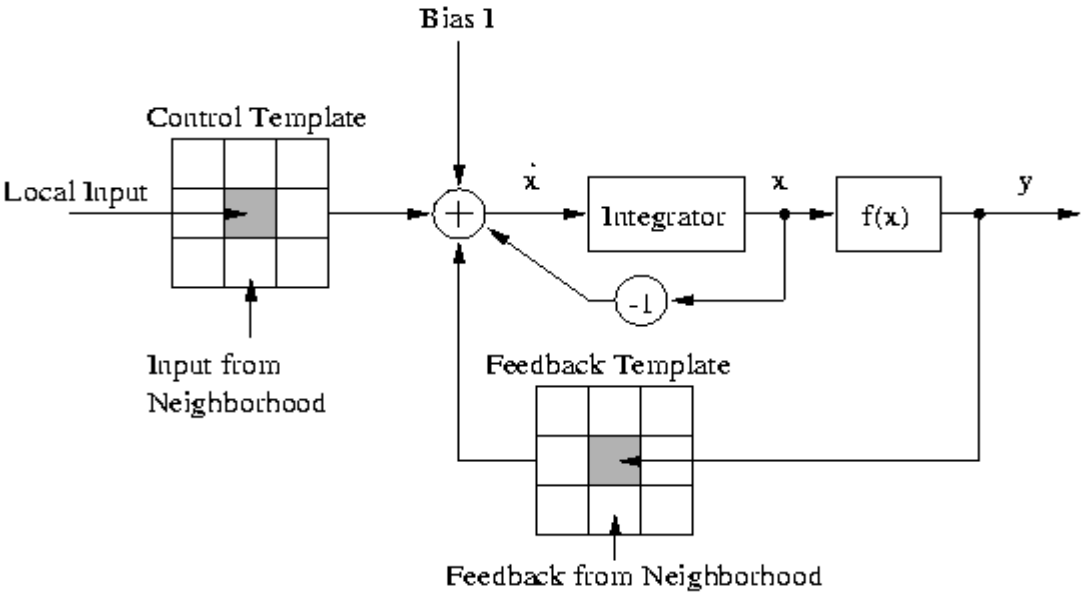

Fig.4 Global behavior of Cellular Neural Networks

ISSN No. 2395-0900
International Journal of
Engineering Studies and Technical Approach
IJESTA

The correlation output corresponding to this input joint image is obtained by Eqs. (3) to (5) as follows

$$
\begin{aligned}
r'(x,z) = {} & [u(x,z)\otimes u(x,z) + y(x,z)\otimes y(x,z) + B(x,z)\otimes B(x,z) + A(x,z)\otimes A(x,z)] \\
& + [\{u(x,z)\otimes B(x,z) + y(x,z)\otimes A(x,z)\} * \delta(z+2z')] \\
& + [\{B(x,z)\otimes u(x,z) + A(x,z)\otimes y(x,z)\} * \delta(z-2z')] \\
& + [\{u(x,z)\otimes y(x,z) + B(x,z)\otimes A(x,z)\} * \delta(x-2x')] \\
& + [\{A(x,z)\otimes B(x,z) + y(x,z)\otimes u(x,z)\} * \delta(x+2x')] \\
& + [A(x,z)\otimes u(x,z) * \delta(x+2x', z-2z') + u(x,z)\otimes A(x,z) * \delta(x-2x', z+2z') \\
& + B(x,z)\otimes y(x,z) * \delta(x-2x', z-2z') + y(x,z)\otimes B(x,z) * \delta(x+2x', z+2z')]
\end{aligned}
\tag{8}
$$

where the first square brackets contain autocorrelation terms of all the objects in the input joint image. The second and third square brackets contain summation of cross-correlations, which are the terms of interest for actual CNN output. The last terms in the brackets are other correlation distributions [9-11].

The zero order terms in Eq. (8) are seen in the correlation output image strongly. Fig. 3 illustrates correlation output imageafter the elimination of zero-order terms by Fourier substraction technique.Then the resulting magnitude square of Eq. (8) is obtained by placing a detector around either $(0,-2y')$ or $(0,2y')$. The actual output image is then produced performing rest of summation operations digitally.

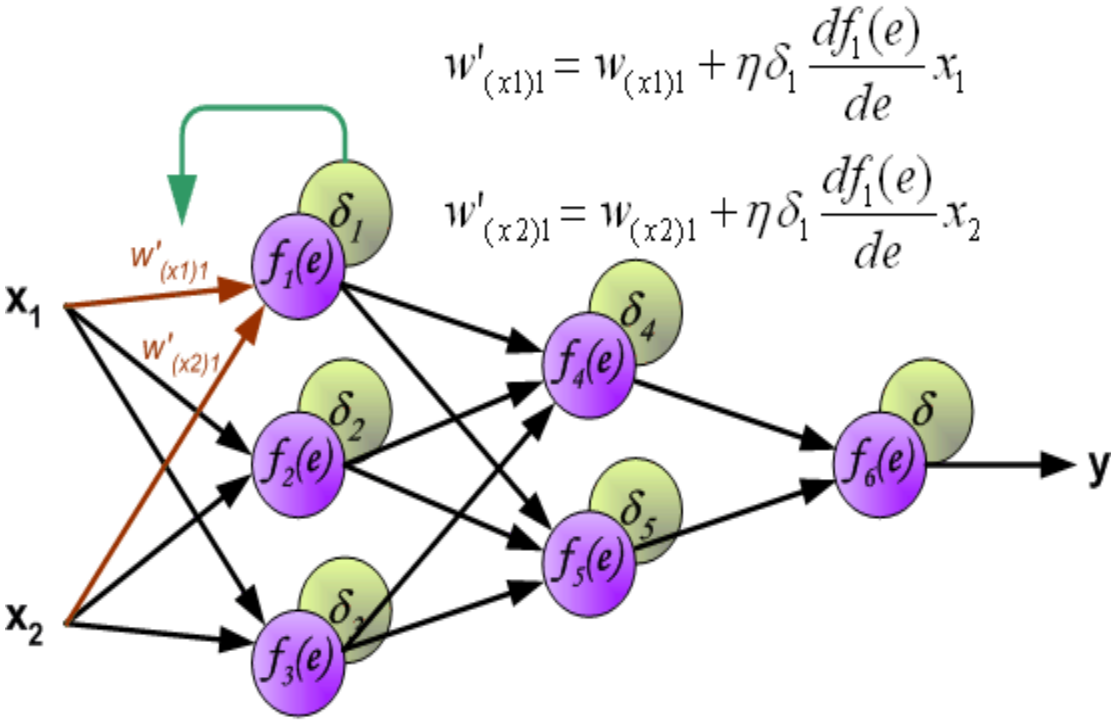

Fig. 5 Correlation output image.

International Journal of Engineering Studies and Technical Approach
IJESTA
ISSN No. 2395-0900

Experimental Results

The experimental study has been conducted on a ASUS-X550C laptop computer with Associate in Nursing Intel Core i3-3217U, 1.8 GHz CPU and 4GB of memory, running in Windows eight.1. All programs square measure coded in Matlab. The dataset T1014D100K that was generated by IBM Quest artificial knowledge Generation. the important world datasets Sina Weibo and Twitter are wont to appraise the INASU. The speed of the planned algorithmic rule is compared with WEAPON and CASINO algorithms by conducting experiments exploitation. The performance of the INASU is healthier than WEAPON and CASINO. Table a pair of explains the Comparison of algorithms - WEAPON,

CASINO and INASU. Fig. one shows the performance analysis of the algorithms that Table a pair of explains in an exceedingly bar . Fig.6 a pair of exhibits the performance analysis of the algorithmic rules exploitation to point out the INASU algorithm higher|is best|is healthier} than WEAPON and CASINO in extracting the small print consistent with the user's want with better speed.

Table 1. Comparative Experimental Results of WEAPON, CASINO and INASU Algorithms

Dataset	Algorithm	Speed Rate
T1014D100K	INASU	0.99
	WEAPON	0.93
	CASINO	0.82
Sina Weibo	INASU	0.97
	WEAPON	0.94
	CASINO	0.79
CNN	INASU	0.99
	WEAPON	0.96
	CASINO	0.84

To evaluate the performance of the proposed optoelectronic learning algorithm for CNN, a detailed simulation program has been developed using MATLAB software package without losing generality. One synthetic image is selected to optimize CNN coefficients for edge detection application. In the first stage, 26x26-pixel an image as shown in Fig. 4(a) is introduced to CNN as input and state image. Desired image is selected edge extracted image of the input image as shown in Fig. 4(b). In the each iteration, CST is employed for summing cross-correlations and the output images are obtained (Fig. 4(c,d,e)). After the adding the bias value digitally, the actual output images are obtained as shown in Fig. 4(f). The training is ended after 1008 iterations when CNN converged to desired output image with minimum error.

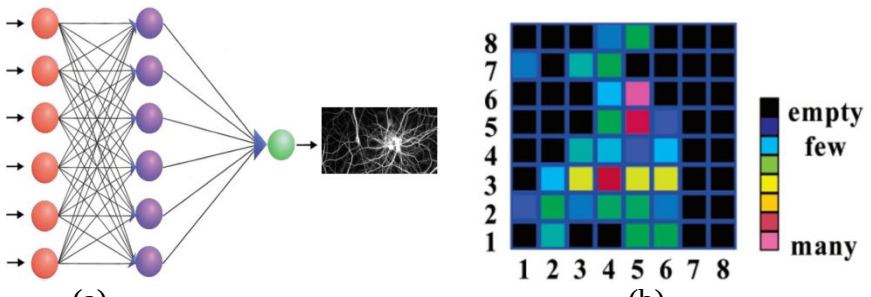

(a) (b)

ISSN No. 2395-0900
International Journal of
Engineering Studies and Technical Approach
IJESTA

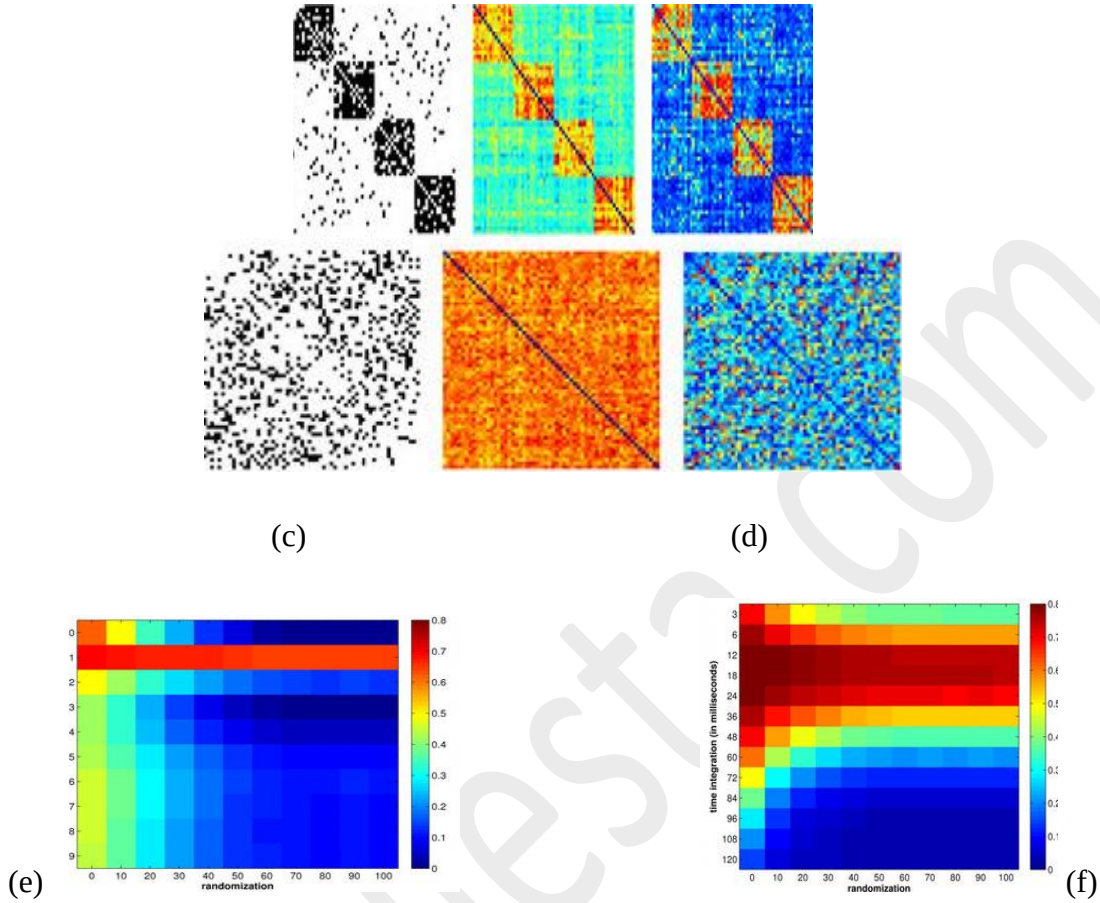

Fig. 6 Output images of optoelectronic learning algorithm for CNN a) Input image, b) Desired output image, c) Output image of iteration # 100, d) Output image of iteration # 500, e) Output image of iteration # 800, f) Output image of iteration # 1008.

Templaste

In image processing, n-by-m rectangular grid arrays are often used. n and m are the numbers of rows and columns, respectively. Each cell in a CNN corresponds to an element of the array.

Assuming that each cell is connected to its nearest neighbors only ("3*3-neighborhood") and that the local connections of a cell do not depend on the cell's position, the Template set contains 19 coefficients (A-Template: a1 .. a9, B-Template: b1 .. b9, Bias I). The behavior of the CNN is completely determined by this Template set.

New CNN-Templates for arbitrary tasks may be found using a training algorithm, or by defining local rules for a given global task. The local rules describe a cell's equilibrium state depending on the inputs and outputs of the neighbor cells. The inputs and the outputs of the neighbor cells are assumed the be constant. The dynamics of the cell is not specified. If Template values for the local rules are found, simulations are very helpful to test the dynamic global behavior of the entire clone of cells.

Global task: Binary edge detection

If the input image is a binary image (black and white), the output of the CNN will be a binary image showing the edges of the input image only. If the input image has intermediate (gray) values, the operation of the CNN with this simple Templaste set is not well defined.

Local rules

Regarding the global tasks, we can define local rules for a single cell. The rules are deduced from the following reflections:
1. A white pixel never turns black.
2. A black pixel turns white if it is surrounded by black pixels
3. A black pixel never turns white, when at least one neighbor cell is white. In this case, this cell belongs to the edge of the object

	Input u(i, j)	Output y(i, j) (t = infinity)
1.	white pixel	white, independent of neighbors
2.	black pixel	white, if all nearest neighbors are black
3.	black pixel	black, if at least one nearest neighbor is white

Table 2 :Experimental Results and INASU Algorithms

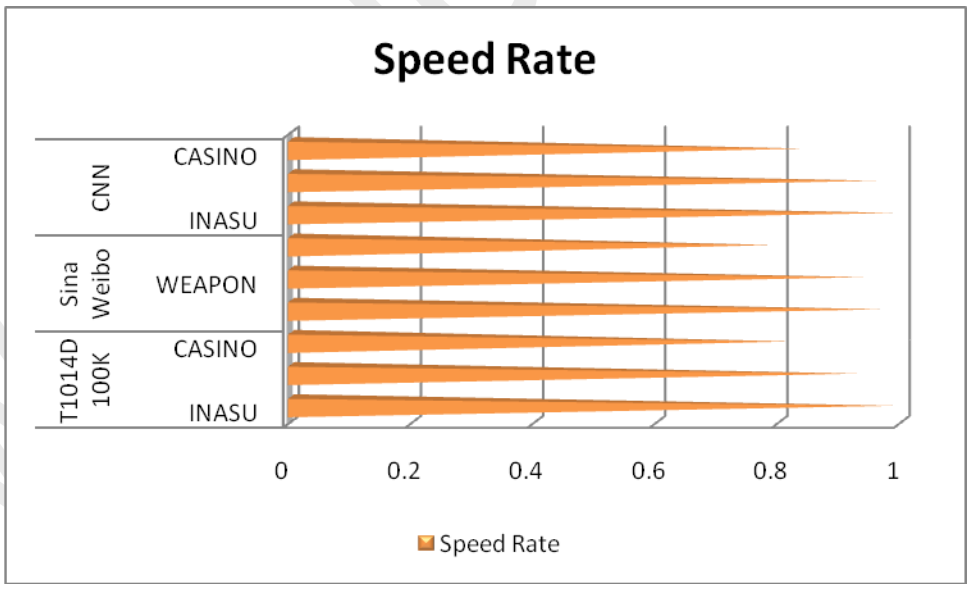

Fig 7. Overall INASU Algorithms Output

CONCLUSION

An optoelectronic coaching method has been enforced for CNN victimization one among the acknowledge optical correlation joint rework correlation. The convolution operation is handled victimization multi-object input joint pictures. Overlapping properties of CST square measure then used for summation of 2 cross-correlations which give less computation advantage for coaching stage. Considering the coaching method needs a lot of computation compared to check method, the projected optoelectronic hardware design offers an alternate implementation chance.

The advantage of the projected hardware implementation is that the ability of incorporation at the same time with varied optical image process or optical pattern recognition techniques simply within the same optical system.

ACKNOWLEDGMENT

This paper is made possible through the help and support from everyone, including: My wife M.suganya and Daughter S.S.Inakshi and My best sir S.Syed Nazimuddeen and in essence, all sentient beings. I sincerely thank to my parents N.Periyasamy and P.Chinnaponnu my brother P.Nallusamy in varagubady village family, and friends, who provide the advice and financial support. The product of this paper would not be possible without all of them.

REFERENCES

i. Pierre Lauret, Frédéric Heymes, Laurent Aprin, Anne Johannet,Atmospheric dispersion modeling using Artificial Neural Network based cellular automata,Environmental Modelling & Software, Volume 85, November 2016, Pages 56-69

ii. Mohammed Salah M'HAMDI, Chaouki AOUITI, Abderrahmane TOUATI, Adel M. ALIMI, Vaclav SNASEL,Weighted pseudo almost-periodic solutions of shunting inhibitory cellular neural networks with mixed delays, Acta Mathematica Scientia, Volume 36, Issue 6, November 2016, Pages 1662-1682

iii. Chuangxia Huang, Jie Cao, Jinde Cao,Stability analysis of switched cellular neural networks: A mode-dependent average dwell time approach,Neural Networks, Volume 82, October 2016, Pages 84-99

iv. Abdujelil Abdurahman, Haijun Jiang, Zhidong Teng,Finite-time synchronization for fuzzy cellular neural networks with time-varying delays,Fuzzy Sets and Systems, Volume 297, 15 August 2016, Pages 96-111

v. Binglong Lu, Haijun Jiang, Abdujelil Abdurahman, Cheng Hu,Global generalized exponential stability for a class of nonautonomous cellular neural networks via generalized Halanay inequalities Neurocomputing, In Press, Corrected Proof, Available online 21 July 2016

vi. Jung-Chao Ban, Chih-Hung Chang,When are two multi-layer cellular neural networks the same?,Neural Networks, Volume 79, July 2016, Pages 12-19

vii. Bingwen Liu,Global exponential convergence of non-autonomous cellular neural networks with multi-proportional delaysNeurocomputing, Volume 191, 26 May 2016, Pages 352-355

viii. Xiaofang Hu, Guanrong Chen, Shukai Duan,A novel memristive cellular neural network with time-variant templates,Perspectives in Science, Volume 7, March 2016, Pages 126-132

ix. Shi-Liang Wu, Tong-Chang Niu,Qualitative properties of traveling waves for nonlinear cellular neural networks with distributed delays,Journal of Mathematical Analysis and Applications, Volume 434, Issue 1, 1 February 2016, Pages 617-632

x. Zhi-Xian Yu, Ming Mei,Uniqueness and stability of traveling waves for cellular neural networks with multiple delays,Journal of Differential Equations, Volume 260, Issue 1, 5 January 2016, Pages 241-267

xi. Shujun Long, Hongheng Li, Yongxin Zhang,Dynamic behavior of nonautonomous cellular neural networks with time-varying delays,Neurocomputing, Volume 168, 30 November 2015, Pages 846-852

xii. Jiangyang Li, Zhenming Peng,Multi-source image fusion algorithm based on cellular neural networks with genetic algorithm,Optik - International Journal for Light and Electron Optics, Volume 126, Issue 24, December 2015, Pages 5230-5236

xiii. M. Kalpana, P. Balasubramaniam,Asymptotical state estimation of fuzzy cellular neural networks with time delay in the leakage term and mixed delays: Sample-data approach,Journal of the Egyptian Mathematical Society, Volume 24, Issue 1, January 2016, Pages 143-150

xiv. Jung-Chao Ban, Chih-Hung Chang,Realization problem of multi-layer cellular neural networks,Neural Networks, Volume 70, October 2015, Pages 9-17

xv. Ani Jiang,Exponential convergence for shunting inhibitory cellular neural networks with oscillating coefficients in leakage terms,Neurocomputing, Volume 165, 1 October 2015, Pages 159-162

xvi. Swati Tyagi, Syed Abbas, Manuel Pinto, Daniel Sepúlveda,Uniform Euler approximation of solutions of fractional-order delayed cellular neural network on bounded intervals,Computers & Mathematics with Applications, In Press, Corrected Proof, Available online 30 April 2016.

xvii. Senthil P. IMAGE MINING USED SEGMENTATION TECHNIQUE MRI SCAN BRAIN TUMOR IMAGES ANALYSIS (IMUSA). Journal of Computer - JoC, Available Online at: www.journal.computer. 2016 Jul 22;1(Volume 1 Issue 1 ISSN:2518-6205):36-50.

xviii. Senthil P. IMAGE MINING EFFECT USING GAUSSIAN SMOOTH IN BRAIN TUMOR INCREASING THE SEGMENTING ACCURACY (I- MENINGIOMA). Journal of Computer - JoC,. 2016 Jul 26;2(Vol.1 Issue. 2, July- 2016):pages-63.

xix. Senthil P. IMAGE MINING CLASSIFICATION MRI SCAN USED BRAIN TUMOR ANALYSIS (IMICLA). Journal of Computer - JoC. 2016 Jul 22;1(Volume 1 Issue 1 ISSN:2518-6205):21-35.

xx. Senthil P. Brain Tumors Frequency Image Mining Used Detection Time Technique in Medical Images. International Journal of Modern Electronics and Communication Engineering (IJMECE) ISSN: 2321-2152 Volume No.-4, Issue No.-3, May, 2016. 2016 Apr 22;4(Volume No.-4, Issue No.-3, May, 2016):39-45.

xxi. Senthil P. Image Mining in Tumor Detection in Brain using Sushisen in Arima Model. Indian Journal Of Natural Sciences. 2016 Sep 3;37(1):Pages-11480.

xxii. Senthil P. EXPOSURE WITH CREDENTIALS OF BRAIN TUMOR USING IMAGE MINING MICCAI PERFORMANCE (MELANOMA). International Journal of Current Research. 2016 Aug;8(Vol. 8, Issue, 08,):Pages-36002.

xxiii. Senthil P. IMAGE MINING USING DISEASE ACCURACY ANALYSIS (Muda). International Research Journal of Engineering and Technology (IRJET). 2016 Aug 16;3(06 June-2016):pages-309.